ORIGINAL ARTICLE

Effect of the feed rate on three-dimensional topography of Ti-6Al-4V based on dynamic mechanical model analysis in cutting process

Jinquan Li[1] · Chenyu Wang[1]

Abstract
The dynamic model of single-degree-of-freedom in cutting vibration system and the tool-tip motion trajectory equation were established by cutting experiment for the titanium alloy (Ti-6Al-4V). The coupling relationships among cutting vibration, cutting force, the unevenness of three-dimensional shape, and feed rate were quantitatively analyzed. The contact area between the tool and the workpiece increases with the increase of the feed rate, which leads to increasing the friction force and the steady-state component of the cutting force. The vibration acceleration increases with the increase of the steady-state component of the cutting force to cause bigger tip displacement, which results in that the surface roughness increases with an increase of the feed rate according to the dynamic model. It can be known from the tool-tip motion trajectory equation that the bigger the feed rate, the bigger the unevenness of three-dimensional shape.

Keywords Feed rate · Cutting force · Cutting vibration · Dynamical model

1 Introduction

Titanium alloys are extensively applied in the aerospace industry with good excellent strength-to-density ratio [1]. However, titanium alloys are difficult to be machined with low thermal conductivity and low modulus of elasticity, which results in high temperatures between the tool and chip to cause rapid tool wear, and increases the static and dynamic deflection with a comparable level of cutting forces. During the cutting process for titanium alloys, excessive vibrations may occur between cutting tool and workpiece to cause worse surface, reduce tool life and processing efficiency, and may damage cutting tool and create noise in the work environment [2, 3]. Therefore, it is of great significance to study the influence of cutting parameters on cutting vibration and analyze the causes of cutting vibration for improving the surface quality of titanium alloys.

The tool vibration is mainly divided into forced vibration resulting from non-cutting factors and self-excited vibration only caused by the cutting process. The study of tool vibration in this paper is only cutting vibration. The cutting force may be produced when tool nose is used to cut the workpiece, which makes cutter bar produce elastic deformation that may restore when the chip is broken. The radial cutting force varies from big to small with the generation and fracture of chips to form a sine wave cutting force with a regular change of size and direction. If the cutting force is large enough, the resonance—i.e., the cutting vibration will produce when the change frequency of the cutting force is equal with natural frequency of process system [4]. Therefore, the methods of eliminating the cutting vibration of tool would include three aspects: (1) The cutting force should be minimized; (2) the static rigidity of tool system should be strengthened as far as possible; (3) disturbing frequency of the exciting force—i.e., cutting force to prevent resonance and eliminate cutting vibration.

At present, the high-speed cutting has been the developing direction of machining technology. In high-speed cutting, instantaneous high-speed impacts between the cutting tool and the workpiece limit the shear to a tiny area to produce serrated chip that can affect chip control [5], aggravate the vibration of tool system, make relative location change between workpiece and cutting tool, and affect machining quality [6–8].

In the overview of the research development of the cutting surface quality, researchers have studied the factors affecting

✉ Jinquan Li
  li_jinquan@163.com

[1] School of Mechanical Engineering, Shenyang Ligong University, No.6 Nanping Center Road, Hunnan New District, Shenyang 110159, People's Republic of China

Table 1 The chemical composition of Ti-6Al-4V (wt%)

Materials	C	Fe	N	O	H	V	Al	Ti
Ti-6Al-4V	0.08	0.3	0.05	0.2	0.01	3.5–4.5	5.5–6.8	Balance

the surface quality in the cutting process from various angles and have obtained a lot of research achievements. The study of the cutting surface quality has mainly concentrated on the selection of cutting tool and cutting parameters, and so on [9]. For cutting parameters, the height of built-up edge increases with the increase of the feed rate, which results in increasing the height of theoretical residual area and makes the machined surface rougher [10]. However, the cutting force and cutting vibration influenced by feed speed and cutting depth will lead to producing the displacement between cutting tool and workpiece, which results in poor surface quality [11]. Therefore, it is difficult to only consider the cutting tool and the optimization of cutting parameters for meeting the technological requirements of high precision and processing stability. In the process of improving the cutting surface quality, it is very necessary to control the cutting force and cutting vibration and consider the cutting dynamic model [12–15]. Meritt [16] predicted cutting vibration stability with cutting depth and chip shape. Mahnama et al. [17] studied the influence of the cutting speed, tool geometry, and the change of shear angle on the cutting vibration and surface quality. A frequency-domain method was used to determine the stable regions between the system displacements and cutting forces [18]. The stable cutting parameters region was predicted by semi-discretization method [19]. Lida Zhu [20, 21] studied the impact of cutting parameters on the surface roughness with orthogonal experiments by establishing two degrees of freedom of the damping system of workpiece. Taylor [22] extensively studied on metal machining and proposed the cutting force model with 3/4 power law. Arnold [23] found that the cutting forces are a function of the cutting speed. Tlusty et al. [24] studied the stability of tool system in the cutting vibration, which the amplitude of dynamic cutting forces rapidly increases to make the cutting process unstable if the cut depth exceeds the

stability limit. Paris [25] found that the dynamic characteristics of the cutting vibration system would affect the quality of the machined surface by using the software to predict the surface topography from the perspective of simulation.

The main factors affecting the cutting force include tool parameters, cutting parameters, tool clamping way, and workpiece material. The reasons affecting the tool vibration are complex are the result of coupling action of various factors. The study must be started with a single factor first in order to figure out the nature of the coupled vibration.

Due to the difficulty for online monitoring of the cutting surface quality, there is no mature theory to study systematically the relationship among cutting force, cutting vibration, and cutting parameters. Therefore, on the basis of previous studies, the influence law of the feed rate on the cutting vibration and cutting surface quality is studied by establishing the dynamic model of workpiece-tool vibration system for Ti-6Al-4V in this paper.

2 Experimental

The single factor dry cutting experiment, only changing the feed rate, was conducted on CA6140 lathe. The Sandvik PVD-coated blades and the annealed Ti-6Al-4V were used. The tool rear angle is $\alpha_0 = 7°$, cutting edge angle is $k_r = 90^0$, rake angle is $\gamma_0 = 7° = 0$, cutting edge inclination is $\lambda_s = 0°$, corner radius is $r_\varepsilon = 0.8$ mm. The compositions are shown in Table 1. The total workpiece length is 300 mm and the diameter is 90 mm. The specimen was divided into several segments with the corresponding cutting parameters (see Table 2 numbered list) along the length of the workpiece. The DYTRAN with a three-direction acceleration sensor was used for the vibration test. The sampling frequency is 10,240 Hz. The cutting force was measured by a piezoelectric three-dimensional dynamometer (YDCB-III05). The arc surface of workpiece was cut by WEDM to measure a three-dimensional shape with a laser scanning confocal microscopy (LSM700). The sensor was directly installed to the cutting tool. The experimental setup is shown in Fig. 1. The experiment scheme,

Table 2 The cutting parameters, root-mean-square of vibration acceleration, and cutting force

Numbered list	Cutting speed (V) (m/min)	Feed rate (f) (mm/r)	Cutting depth (a_p) (mm)	Vibration acceleration (g)	Cutting force (N)
1	97	0.10	0.2	0.2413	80.511
2	97	0.15	0.2	0.3299	91.711
3	97	0.20	0.2	0.3945	98.172
4	97	0.24	0.2	0.4468	112.095
5	97	0.30	0.2	0.5737	125.813

Fig. 1 The experimental setup for testing

Experimental setup
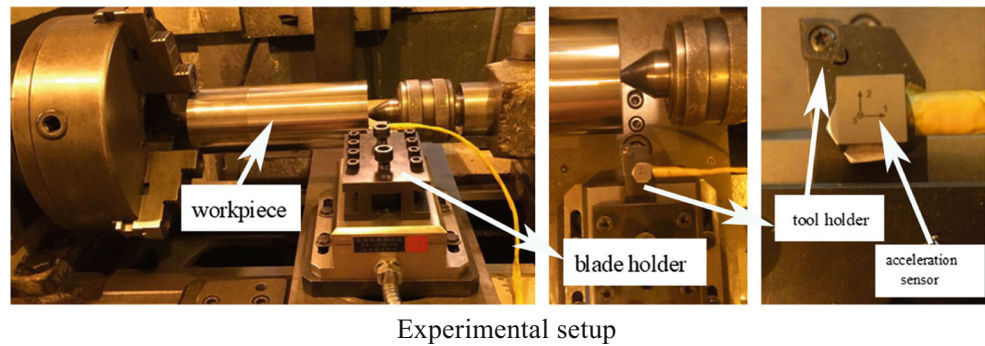
the value of the root-mean-square of vibration acceleration, and cutting force component are shown in Table 2. The characteristic parameters of the three-dimensional topography, stable cutting force, and the amplitude of vibration acceleration are respectively shown in Tables 3 and 4. The metallographic specimens were made to observe chip microstructure by metallurgical microscope.

3 Results and discussion

3.1 The characteristics of surface three-dimensional morphology affected by the feed rate

Figure 2 shows the three-dimensional topography of the surface contour for Ti-6Al-4V in different feed rates. The x-direction coordinate represents the distance between adjacent crest and trough, the y-direction represents the width of the sample, and the z-direction coordinate represents surface waviness. The characteristic parameters representing the three-dimensional topography of surface contour (i.e., Fig. 2a, b, c, and d) increase with the increase of the feed rate, as shown in Table 3.

3.2 The characteristics of cutting vibration and cutting force affected by the feed rate

Figure 3 shows the time domain of tool vibration acceleration obtained by the single factor experiments of only changing the feed rate for Ti-6Al-4V. Figure 4 shows the change of root-mean-square of vibration acceleration with the feed rate. It can be seen from Figs. 3 and 4 that the vibration acceleration increases with the increase in the feed rate.

Figure 5 shows that the cutting forces change with time under different feed rates for Ti-6Al-4V. Figure 6 shows that the root-mean-square of the cutting force change with the feed rate. The cutting forces increase with the increase of feed rates.

3.3 The shape of the serrated chip

Figure 7 a, b, c, and d shows the chip shapes produced by different feed rates with the constant cutting speed and cutting depth for Ti-6Al-4V. The serrated chips spaced evenly by adiabatic shear band (ASB), just like the white arrows are pointing in Fig. 7d, were produced under different feed rates. The degree of serration increased with an increase in the feed rate. The difference of the chip shape presents different chip deformation degrees during machining, which adiabatic shear failure plays a leading role for a Ti-6Al-4V chip.

3.4 The influence of the feed rate on the dynamic system in the cutting process

The physical model of the cutting vibration can be described below: the tool system is considered as a combination of massless spring k and inelastic mass block m with an inherent frequency. The m oscillates with the sine wave around their equilibrium positions under the repeated action of the cutting force. The cutting vibration occurs when the frequency of the cutting force is equal to or near to the natural frequency of the

Table 3 The characteristic parameters of three-dimensional topography of Ti-6Al-4V surface profile

Feed rate f (mm/r)	Arithmetic mean deviation Pa (μm)	Root-mean-square deviation Pq (μm)	Maximum profile peak height Pp (μm)	Maximum profile valley depth Pv (μm)	Total height of profile Pt (μm)	Interfacial spread area ratio Sdr (%)
$f = 0.1$	1.699	2.107	4.063	4.000	9.064	0.446
$f = 0.15$	1.763	2.252	4.101	5.581	9.956	0.601
$f = 0.2$	1.784	2.274	4.374	6.196	10.297	0.669
$f = 0.3$	4.386	5.217	11.291	9.232	20.523	1.506

Table 4 The stable cutting force component F_f, vibration acceleration amplitude A

f (mm/r)	0.10	0.15	0.20	0.24	0.30
$F_f(N)$	78.217	86.568	90.829	109.739	119.326
A(g)	0.1182	0.1222	0.2008	0.2174	0.3222

tool system, which is attenuation process under the action of gravity and air resistance. Therefore, the model of single-degree-of-freedom of the cutting system is shown in Fig. 8a. Figure 8b is the partial enlargement of the machined surface. Figure 8c is the principle models in cutting.

The tool vibration equation of the single-degree-of-freedom is as follows:

$$m\ddot{x}(t) + c\dot{x}(t) + kx(t) = -F(t) \qquad (1)$$

where m is the tool system mass, $m = 1.036$ kg, c is damping, $c = 345$ N/(m/s), k is the rigidity of tool compressed by workpiece, and $k = 281,333,529$ N/m [26].

The cutting force $F(t)$ in a time domain signal is composed of two parts: one is the steady-state cutting force component close to the measured mean value of cutting force; the other is the dynamic cutting force component of the sinusoidal function fluctuating around the steady-state cutting force [27]. That is,

$$F(t) = F_f + F\sin(\omega t + \phi) \qquad (2)$$

where F_f is the steady-state cutting force component, $F\sin(\omega t + \phi)$ is the dynamic cutting force component.

The empirical formula for the cutting force affected by the feed rate is as follows:

$$F_f = C_f \cdot a_p^{x_{Fc}} \cdot f^{y_{Fc}} \qquad (3)$$

where C_f is the coefficient of cutting force affected by material hardness, y_{Fc} is the index of the feed rate f, x_{Fc} is the index of cutting depth a_p. Therefore,

$$F(t) = C_f \cdot a_p^{x_{Fc}} \cdot f^{y_{Fc}} + F\sin(\omega t + \phi) \qquad (4)$$
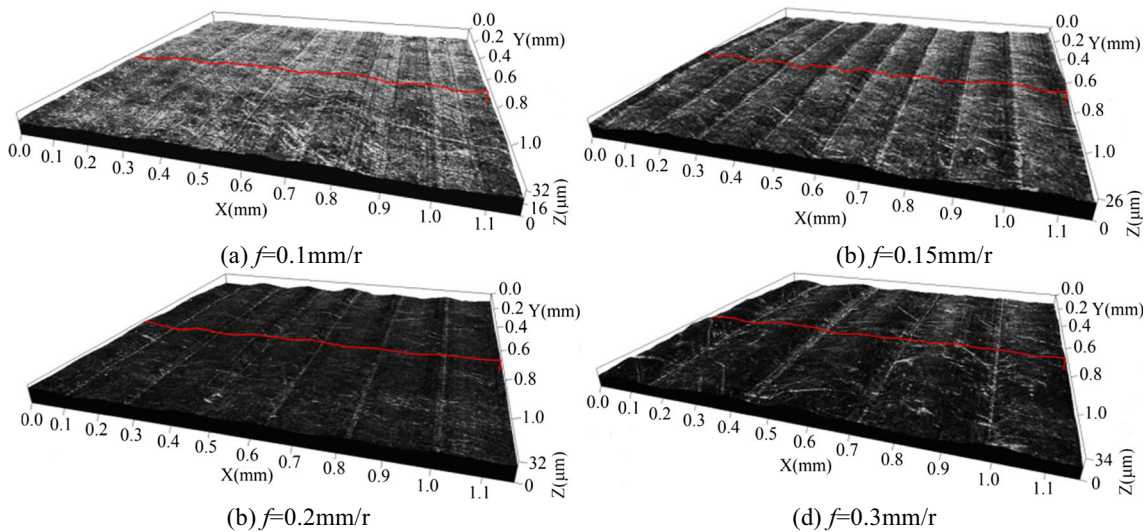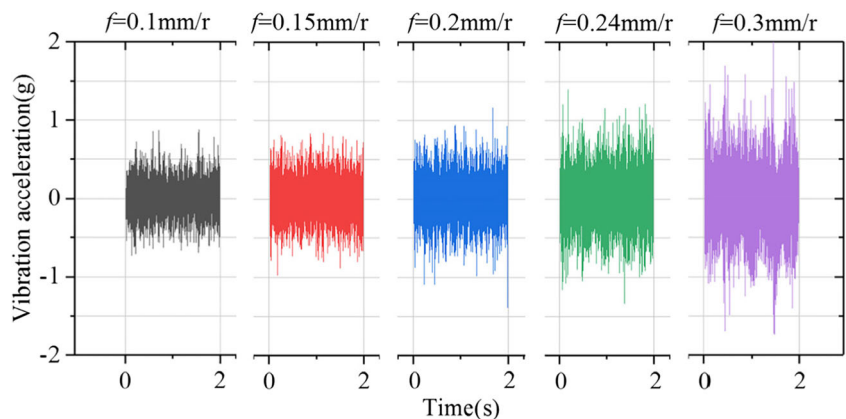

Fig. 2 Three-dimensional topography of Ti-6Al-4V surface profile in different feed rates: **a** $f = 0.1$ mm/r; **b** $f = 0.15$ mm/r; **c** $f = 0.2$ mm/r; **d** $f = 0.3$ mm/r

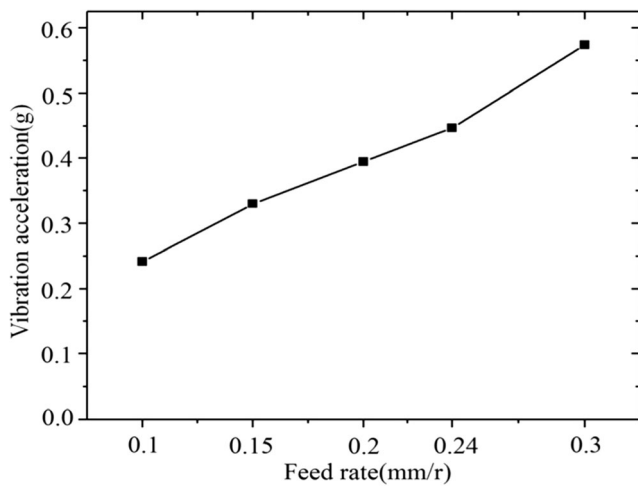**Fig. 3** The time domain of tool vibration acceleration with changing feed rate

Fig. 4 The tool vibration characteristics with changing the feed rate
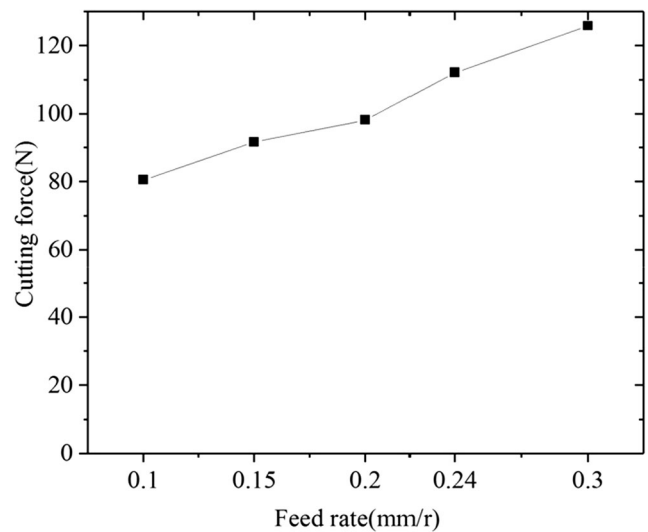

Fig. 6 The cutting force with changing the feed rate

The dynamic cutting force component changes very little relative to the steady-state cutting force component, therefore, $F, \omega,$ and ϕ are approximately set as constant.

By fitting cutting force data (including F_f value in Table 4) collected by the experiment with Eq. (2) and Eq. (4), these parameters can be obtained as follows:

C_f=961, x_{Fc}=1, y_{Fc}=0.413, F=5.695, ω=15,319.98, ϕ= − 1.055. Therefore,

$$F(t) = 192.2 \cdot f^{0.413} + 5.695\sin(15319.98t - 1.055) \quad (5)$$

Origin software is used to draw the function image of Eq. (5), as shown in Fig. 9. The time function of cutting force increases with the increase in the feed rate shown in Fig. 9.

Substitute Eq. (5) into Eq. (1) to get the following:

$$m\ddot{x}(t) + c\dot{x}(t) + kx(t) = -[F_f + F\sin(\omega t + \phi)] \quad (6)$$
$$= -[192.2 \cdot f^{0.413} + 5.695\sin(15319.98t - 1.055)]$$

The vibration acceleration response with the time under different feed rates can be obtained by taking the second derivative with respect to $x(t)$ in Eq. (6), which gradually

attenuated to zero due to damping, as shown in Fig. 10. The vibration acceleration increases with the increase of the feed rate (Fig. 10). It can be seen from Eq. (6) that the steady-state component of cutting force $F(f)$ increases with the increase of the feed rate to result in increasing cutting vibration acceleration $\ddot{x}(t)$.

In the cutting process, the workpiece surface is cut by arc cutting edge of tool tip to form the surface topography with different microscopic unevenness. R_{max} is the maximum height of the residual area, as shown in Fig. 8b. According to the geometric relationship in Fig.8b, the express of R_{max} is as follows:

$$R_{max} = r - \sqrt{r^2 - \left(\frac{f}{2}\right)^2} \quad (7)$$

where r is corner radius of the tool tip. The R_{max} increases with the increase in the feed rate.

Ideally, the center point of the corner radius of the tool tip is (x_0, z_0), $z_0 = 0$, a point on the machined surface is (x, z), $z(t) = r - \sqrt{r^2 - (x - x_0)^2}$, as shown in Fig. 8b. But the radial

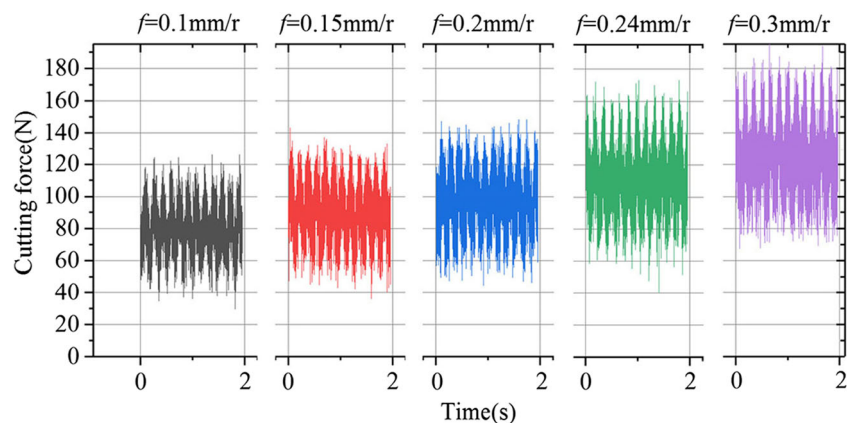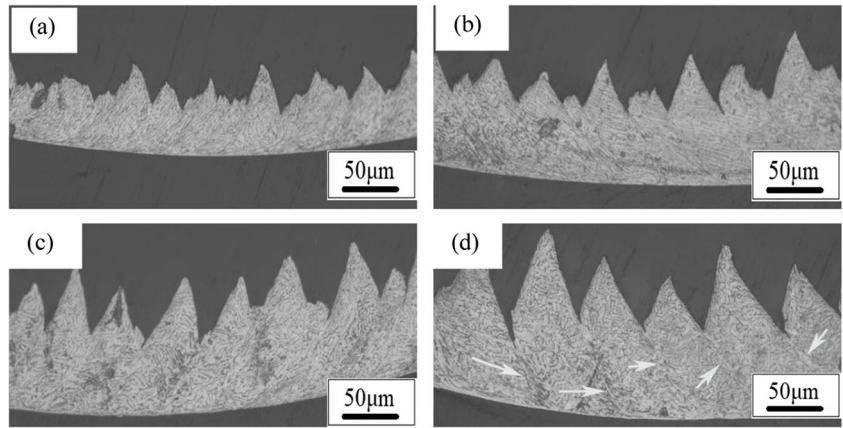Fig. 5 The time domain of cutting force with changing the feed rate

Fig. 7 The chip shape of Ti-6Al-4V (v = 97 m/min, a_p = 0.2 mm). **a** f = 0.15 mm/r; **b** f = 0.2 mm/r; **c** f = 0.24 mm/r; **d** f = 0.3 mm/r

displacement of the tool tip will be produced by cutting vibration in actual cutting process. The radial displacement under different feed rates is set as Zr(t). In this case, z_0 = Zr(t),

$$z(t) = r - \sqrt{r^2 - (x - x_0)^2} + \text{Zr}(t).$$

Therefore, the movement track equation of tool tip is as follows:

$$\begin{cases} x(t) = V_f \cdot t = \dfrac{f \cdot n}{60} \cdot t \\ z(t) = r - \sqrt{r^2 - (x - x_0)^2} + \text{Zr}(t) \end{cases} \quad (8)$$

where V_f is the feed speed, n is the spindle speed, $x(t)$ is the displacement of the tool tip in the feed direction, and $z(t)$ is the radial displacement. In order to calculate Zr(t), the sine function $g(t) = A\sin(\omega t + \phi)$ is used to fit the vibration acceleration data along the radial direction tested by cutting test. The fitting expression of vibration acceleration is as follows:

$$g(t) = A\sin(15707t + 314.16) \quad (9)$$

where A is the amplitude of vibration acceleration. The A value is shown in Table 4.

Fig. 8 The analytical model of the cutting process: **a** the model of single-degree-of-freedom of the cutting system, **b** the partial enlargement of the machined surface, **c** the principle models in cutting
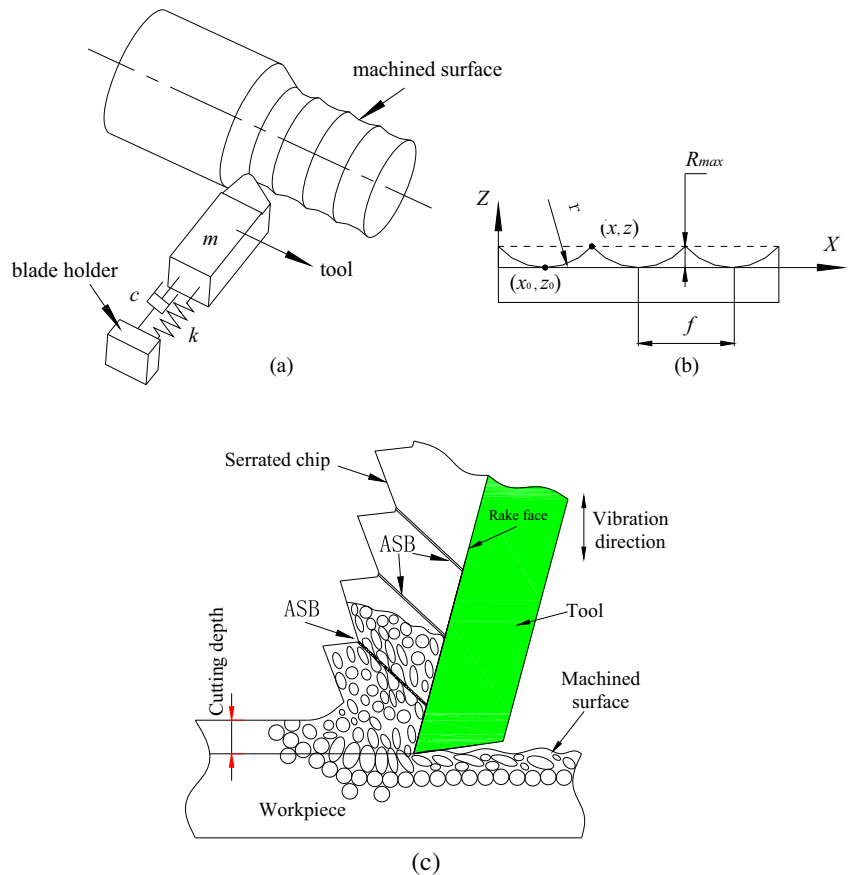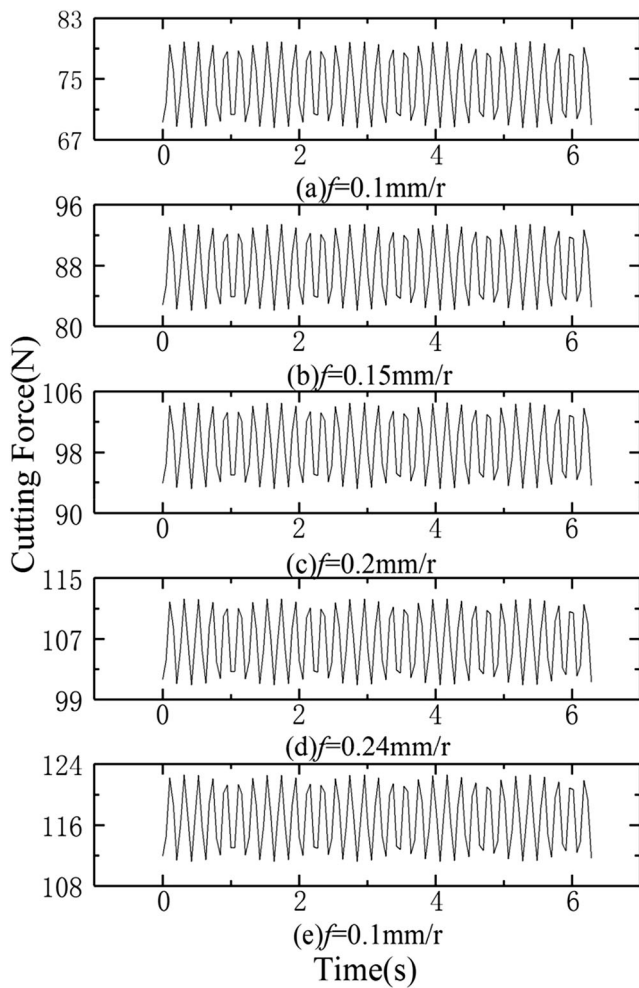
Fig. 9 The function image of $F(t)$

Fig. 10 The transient response of vibration acceleration

In integral interval [0-t], the double repeated integral of $g(t) = A \sin(\omega t + \phi)$ can be obtained as follows:

$$Zr(t) = A\left[\frac{t}{\omega}\cos\phi - \frac{1}{\omega^2}\sin(\omega t + \phi) + \frac{1}{\omega^2}\sin\phi\right] \quad (10)$$

ω and ϕ are set up to be constant value because they are little changed with the change of the feed rate. The value of A increases with the increase of the feed rate, as shown in Table 4.

Substituting Eq. (10) into Eq. (8), the equation of the movement track of tool tip influenced by vibration acceleration amplitude A and the feed rate f is obtained as follows:

$$\begin{cases} x(t) = \dfrac{f \cdot n}{60} \cdot t \\ z(t) = r - \sqrt{r^2 - (x-x_0)^2} + A\left[\dfrac{t}{\omega}\cos\phi - \dfrac{1}{\omega^2}\sin(\omega t + \phi) + \dfrac{1}{\omega^2}\sin\phi\right], t \geq 0 \end{cases} \quad (11)$$

It can be known from Eqs. (6), (7), and (11) that all of the vibration acceleration $\ddot{x}(t)$, cutting force $F(f)$, the maximum
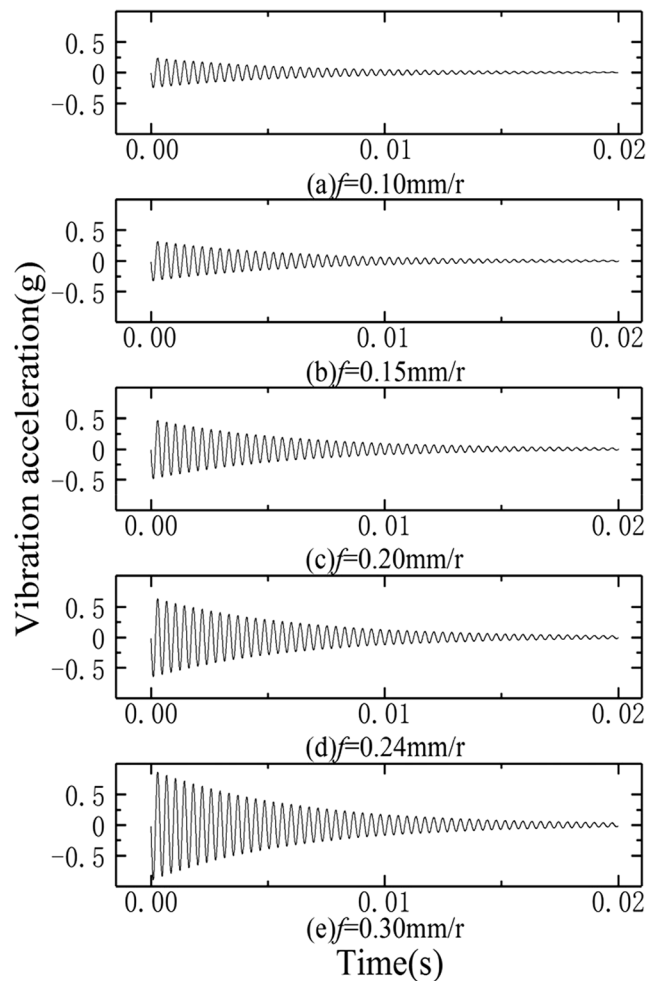
height of residual area R_{max}, and the displacement of tool tip $Z(t)$ increase with the increase of the feed rate. The cutting vibration caused by cutting force in the cutting process will result in the increase of $Z(t)$, which causes the deviation of the feed rate and makes the machined surface rougher. Therefore, the various characteristic parameters (Table 3) representing fluctuation of the three-dimensional shape of the machining surface (Fig.2) in Z-direction increase with the increase of the feed rate, i.e., the surface roughness increases. In the meantime, the contact area between the tool and the workpiece increases with the increase of the feed rate f, which produces tool deformation reacting on the workpiece to result in the unevenness of machining surface.

In addition, the tool has a feed movement along the axis direction while the workpiece rotates in the cutting process, the grooves similar to spiral cut by cutting edge are inevitably produced on the machining surface, and the feed rate is equivalent to screw pitch. Therefore, the distance between adjacent crests and troughs of the uneven surface topography along the feed direction is approximately equal to the feed rate under

ideal state without considering vibration. The bigger the feed rate, the bigger the unevenness of the three-dimensional shape. The interaction between the tool and the workpiece will produce chatter mark on the workpiece surface, which also has a great impact on the surface quality [28].

The serrated chip can occur easily in cutting process for Ti-6Al-4V. Proceeding from a mechanism of producing the serrated chip, the plastic work resulting from the plastic deformation with a strain hardening effect in the primary deformation zone can be converted into heat to cause temperature rise and thermal softening effect. The strain hardening effect and thermal softening effect proceed simultaneously. When the thermal softening effect exceeded the strain hardening effect, the energy barrier accumulated by the plastic work in the local area of the primary deformation zone would be overcome [29], which produced a local thermoplastic shear instability, to produce ASB. After forming ASB, the energy was released in an instant, but the plastic work continued to accumulate and then the next ASB would occur by repeating the above process—i.e., the strain hardening effect and thermal softening effect appeared alternately, to form the serrated chip spaced evenly by ASB, which acted on the rake face of the tool (Fig. 8c) to inevitably resulted in the cutting force vibrate high-frequently. The higher the feed rate, the more prone to producing the serrated chip, the bigger the degree of serration (Fig. 7), and the more seriously the vibrate high-frequently. Therefore, the serrated chip relates to the tool vibration acceleration, which deteriorates surface quality.

4 Conclusions

(1) The contact area between the tool and the workpiece increases with the increase of the feed rate, which leads to the increase of the friction force and the increase of the steady-state component of the cutting force.

(2) The vibration acceleration increases with the increase of the steady-state component of the cutting force, which results in increasing characteristic parameters of the three-dimensional topography according to the dynamic model of single-degree-of-freedom in the cutting vibration system.

(3) The tool-tip motion trajectory equation was established, which shows that the change of the tool-tip position caused by the cutting vibration and the feed rate makes the machined surface rougher.

References

1. Destefani JD (1990) Introduction to titanium and titanium alloys, properties and selection, nonferrous alloys and special-purpose materials, vol 2. ASM Handbook. Materials Park, OH:ASM International
2. Quintana G, Ciurana J (2011) Chatter in machining processes: a review. Int J Mach Tools Manuf 51(5):363–376
3. Cedergren S, Frangoudis C, Archenti A, Pederson R, Sjöberg G (2016) Influence of work material microstructure on vibrations when machining cast Ti-6Al-4V. Int J Adv Manuf Technol 84:2277–2291
4. Landberg P (1956) Vibrations caused by chip formation. Microtechnic 10(5):219–228
5. Li J-q, Zhang R, Guo H-l, Zhang Z-j (2016) Study on chip failure mechanism in high-speed cutting process with electronic theory. Int J Adv Manuf Technol 84:2257–2264
6. Li J-q, Li P, Guo H-l, Zhang Z-j (2017) Study on the formation mechanism of saw-tooth chip in high-speed cutting process. Proc Inst Mech Eng B J Eng Manuf 231(14):2577–2584
7. Komanduri R, Hou ZB (2002) On thermoplastic shear instability in the machining of a titanium alloy (Ti-6Al-4V). Metall Mater Trans A Phys Metall Mater Sci 33(9):2995–3010
8. Khrais SK, Lin YJ (2007) Wear mechanisms and tool performance of TiAlN PVD coated inserts during machining of AISI 4140 steel. Wear 262:64–69
9. Ezugwu EO, Bonney J, Yamane Y (2003) An overview of the machinability of aeroengine alloys. J Mater Process Technol 134:233–253
10. Gong Y, Liang C, Li Q, Liu M (2018) Wear experiment of carbide tool for milling nickel-based single crystal superalloy DD5. J Northeast Univ: Nat Sci Ed 39(09):1283–1287+1326
11. Devillez A, Dudzinski D (2007) Tool vibration detection with eddy current sensors in machining process and computation of stability lobes using fuzzy classifiers. Mech Syst Signal Process 21(1):441–456
12. Bashir BM, Wan M, Liu Y, Yuan H (2018) Active damping of milling vibration using operational amplifier circuit. Chinese Chin J Mech Eng-En 31(05):58–65
13. Lalwani DI, Mehta NK, Jain PK (2008) Experimental investigations of cutting parameters influence on cutting forces and surface roughness in finish hard turning of MDN250 steel. J Mater Process Technol:167–179
14. Peng C, Wang L, Liao TW (2015) A new method for the prediction of chatter stability lobes based on dynamic cutting force simulation model and support vector machine. J Sound Vib 354(10):118–131
15. Turkes E, Orak S, Neseli S, Yaldiz S (2011) Linear analysis of chatter vibration and stability for orthogonal cutting in turning. Int J Refract Met Hard Mater 29(2):163–169
16. JHE M (1965) Theory of self-excited machine–tool chatter. Trans ASME J Eng Indust 87:447–454
17. Mahnama M, Movahhedy MR (2010) Prediction of machining chatter based on FEM simulation of chip formation under dynamic conditions. Int J Mach Tools Manuf 50(7):611–620
18. Altintas Y, Budak E(1995) Influence of Secondary Factors of Spindle Geometry on the Dynamic Stability in End-milling Operation. Annals of CIRP- Manufacturing Technology 44:357–362
19. Insperger T, Stepan G (2002) Int J Numer Methods Eng 55:503
20. Zhu L, Liu B, Chen H (2018) Research on chatter stability in milling and parameter optimization based on process damping. J Vib Control 24(12):2642–2655
21. Zhu L, Li H, Wang W (2013) Research on rotary surface topography by orthogonal turn-milling. Int J Adv Manuf Technol 69:2279–2292

22. Taylor FW (1907) On the art of cutting metals. Trans ASME 28:31–350
23. Arnold RN (1946) The mechanism of tool vibration in the cutting of steel. Proc Instn Mech Eng 154:261–284
24. Tlusty J, Polacek M (1963) The stability of machine tools against self-excited vibrations in machining. Int Res Prod Eng 465–474
25. Paris H, Peigne G, Mayer R (2004) Surface shape prediction in high speed milling. Int J Mach Tool Manu 44(15):1567–1576
26. Benwen XU, Qunying JIAO, Mechanical (1998) Vibration and modal analysis. Machinery Industry Press, Beijing, pp 5–11
27. QIU J (2019) Research on cylindrical turning process stability judgment based on dynamic cutting process. J Mech Eng 55(3):208–218
28. Liu B, Zhu L, Dun Y, Liu C (2017) Investigation on chatter stability of thin-walled parts in milling based on process damping with relative transfer functions. Int J Adv Manuf Technol 89:2701–2711
29. Li J-q, Xu B-c (2017) Study on adiabatic shearing sensitivity of titanium alloy in the process of different cutting speeds. Int J Adv Manuf Technol 93:1859–1865